Induction of oligodendrogenesis with OCT4 to alleviate dysmyelination in a transgenic mouse model of Huntington's disease

MinGi Kim

Department of Medical Science

The Graduate School, Yonsei University

Induction of oligodendrogenesis with OCT4 to alleviate dysmyelination in a transgenic mouse model of Huntington's disease

MinGi Kim

Department of Medical Science

The Graduate School, Yonsei University

Induction of oligodendrogenesis with OCT4 to alleviate dysmyelination in a transgenic mouse model of Huntington's disease

Directed by Professor Sung-Rae Cho

The Master's Thesis
submitted to the Department of Medical Science,
the Graduate School of Yonsei University
in partial fulfillment of the requirements for the degree of
Master of Medical Science

MinGi Kim

June 2018

This certifies that the Master's
Thesis of MinGi Kim is approved.

Thesis Supervisor: Sung-Rae Cho

Thesis Member: Philhyu Lee

Thesis Member: Hyongbum Kim

The Graduate School
Yonsei University

June 2018

ACKNOWLEDGEMENTS

It has been years since I have been entered this laboratory and studied under my supervisor, Sung-Rae Cho. When I started my research, it seemed like I was doing an endless work and never be done. Despite what I have been thinking, time flies, and now it is the final period of my degree.

Here I would like to give my truthful appreciation to my professors. Due to the great guide from my profession Sung-Rae Cho, and thesis Philhyu Lee and Hyongbum Kim, my research reach to the conclusion.

Moreover, I am truly and deeply thanks to my colleges at the lab—Jung Hwa Seo, Suk-Young Song, Ji Hea Yu, Soohyun Wi, Ahreum Baek, Yoon-Kyum Shin, Eunju Cho, Baegeun Nam, and Soonil Pyo. As friends, as seniors and/or as coworkers, they are so much helpful and supported to my both personal and working life.

Among them all, I would like to give the best appreciation to my parents and other family members, who take care beside me and give a courage to approach the final goal. Because of the comfort that my mother and father provided to me, I could focus only in my research

Because of their kind and warm supports, this paper could be done and write the final period on my paper.

After all these years, I finally would like to welcome my future, and now, I can finally say this... “it was a great pleasure to have the time and opportunity in the research.”

June 2018

Kim, MinGi

TABLE OF CONTENTS

LIST OF FIGURES

LIST OF TABLES

ABSTRACT

Induction of oligodendrogenesis with OCT4 to alleviate dysmyelination in a transgenic mouse model of Huntington's disease

MinGi Kim

Department of Medical Science
The Graduate School, Yonsei University

(Directed by Professor Sung-Rae Cho)

Huntington's disease (HD) is an incurable neurodegenerative disease which is caused by a genetic mutation. Recent studies have elucidated that white matter atrophy is an early symptom of HD. Therefore, this study used in vivo overexpression of OCT4, a reprogramming factor, as a treatment for dysmyelination in HD. Adeno-associated virus serotype 9 (AAV9) was used as a vector for the overexpression of OCT4. Each group of R6/2 mice was injected with PBS, AAV9-Null, or AAV9-OCT4 on both

sides of the lateral ventricles. According to the results of the behavioral tests such as rotarod and grip strength tests, AAV9-OCT4 groups display significant improvement compared to control groups—PBS and AAV9-Null. Levels of RNA expression were significantly increased in PDGFRa, WNT3, MYFR and GDNF. In addition, both Nestin+BrdU+ and NG2+BrdU+ cells were increased in the AAV9-OCT4 group compared to the control groups in the subventricular zone. Moreover, the level of MBP protein is significantly increased in AAV9-OCT4 in the frontal cortex. Cumulatively, these results suggest that oligodendrogenesis was induced by in vivo overexpression of a reprogramming factor OCT4 in the subventricular zone, so dysmyelination was alleviated. Furthermore, a growth factor such as GDNF secretion from oligodendrocyte improves the environment in the brain in HD; therefore, behavioral improvement occurred in the R6/2 mouse. Thus, this study proposes OCT4 as a candidate of a therapeutic factor for neurodegenerative diseases including HD.

Key words: Huntington's disease, Neurodegenerative disease, Reprogramming factor, OCT4, Subventricular zone, Oligodendrogenesis, Oligodendrocyte, Dysmyelination

Induction of oligodendrogenesis with OCT4 to alleviate dysmyelination in a transgenic mouse model of Huntington's disease

MinGi Kim

Department of Medical Science
The Graduate School, Yonsei University

(Directed by Professor Sung-Rae Cho)

I. INTRODUCTION

Huntington's disease (HD) is an incurable neurodegenerative disease. Previous studies have reported that the loss of GABAergic neurons is a critical cause of striatal atrophy that drives cognitive and motor impairments in HD.[1,2] For this reason, striatal atrophy has been widely studied.[2,3]

HD should not be simply considered as a striatal disease though the striatal neurons are specially affected since there are many evidences of the degeneration throughout the overall regions of the brain until the later stages of disease.[4] Recent studies have strived to elucidate the effects of white matter atrophy in HD since white matter is affected before the striatal atrophy occurrs.[5-7] Moreover, structural MRI or pathological examinations have been used for diagnosing the pathogenesis in HD brains, and defects of oligodendrocytes and white matter have been detected via these methods in the brains.[5,7-14] The volume of white

matter is noticeably reduced long before the motor onset in HD[13,15-19] and atrophy continues into the manifest period.[13,20,21] The white matter atrophy also has been shown in longitudinal studies in 1–2-year periods in premanifest HD[22,23] and early manifest HD.[24,25] The TRACK-HD group using Statistical Parametric Mapping methodology [25] found that the most important changes in white matter occurred around the striatum and within the corpus callosum and posterior white matter tracts.[26] Aylward et al., elucidated that there is the dramatic volume changes in the frontal lobe using lobular regions of white matter.[5,27] Even though the precise nature of these abnormalities has not been proven, postmortem and neuroimaging data, such as MIR, support the hypothesis that myelin breakdown leads to white matter atrophy in HD.[28]

To alleviate the dysmyelination in white matter, this study overexpressed the reprograming factor to induce the adult oligodendrogenesis in HD. The four factors—octamer-binding protein, (OCT4), SRY-box containing gene 2 (SOX2), c-myelocytomatosis oncogene (c-Myc), and Kruppel-like factor 4 (Klf4)—are widely known as the reprograming factors, and these four factors have been used for the therapeutic factors in brain related diseases.[29,30] Among these four factors, characteristics of OCT4 that induce self-renewal and pluripotency in cells can be more efficient than others. The study by Kim et al. in 2009 reported that OCT4 induced pluripotency in adult neural stem cells.[31] According to the aforementioned studies, OCT4 could be an essential factor for adult oligodendrogenesis. Another study reported that OCT4-induced oligodendrocyte

progenitor cells enhanced functional recovery in spinal cord injury model.[32] To recovery of myelination could be the direct recovery of axonal impairment caused by demyelination.

Thus, a strategy of this study is the inducing of oligodendrogenesis in the subventricular zone and increase the number of oligodendrocyte with myelin with OCT4. Therefore, the study used a single factor of OCT4 as a candidate of the therapeutic factor for demyelinating the condition in various neurodegenerative diseases including HD.

II. MATERIALS AND METHODS

All animals were housed in a facility accredited by the Association for Assessment and Accreditation of Laboratory Animal Care and provided food and water ad libitum with alternating 12-hour light/dark cycles in according with animal protection regulations. The experimental procedures were approved by the Institutional Animal Care and Use Committee (IACUC 2016-0298).

1. Mouse model

One of the well-known transgenic mouse models for HD is B6CBA-Tg(HDexon1)62Gpb/1J, which is also known as B6CBA-R6/2 (CAG 160 +/- 5) (R6/2). These transgenic mice mimic human HD with many neurological phenotypes, including choreiform-like movements, involuntary stereotypic movements, tremor, and epileptic seizures, as well as non-movement disorder components, including unusual vocalization. The R6/2 mice often urinate, and the loss of body weight is the one of the significant characteristics. Their muscle bulk occur through the course of the disease. This line is transgenic for the 5' end of the human HD gene carrying approximately 160 +/- 5 repeat expansions. The symptoms of this mouse onset between 6 and 8 weeks of age.

2. Viral vector

Adeno-associated virus serotype 9 (AAV9) was used to overexpress human octamer-binding transcription factor 4 (OCT4) in vivo. Productions of AAV9 were purchased from ViroVek (Hayward, CA, USA). AAV9 with human OCT4 was expressed by cytomegalovirus (CMV) promotor, AAV9-CMV-OCT4. The

original titer of the virus was 2.13E+13vg/ml, and the titer was measured via quantitative real-time reverse transcription polymerase chain reaction (qRT-PCR).

(A)

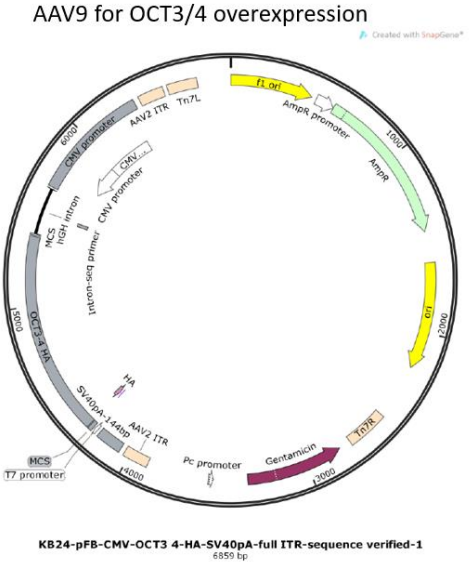

(B)

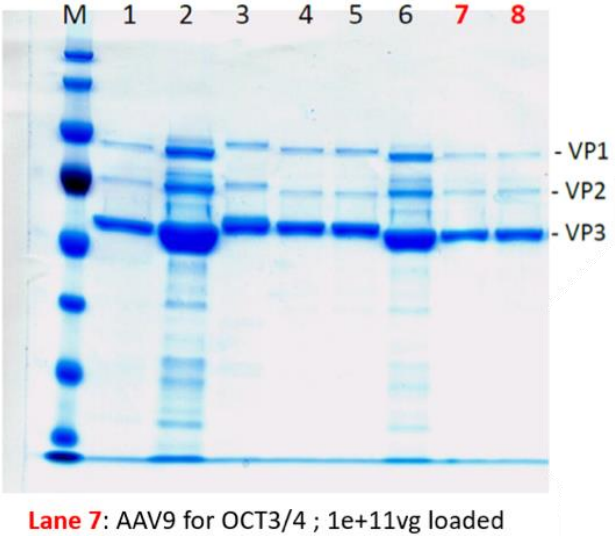

Figure 1. Information about the viral vector for the experiment (A) The structure of the viral vector for overexpressing OCT4 in vivo was referenced from Snap Gene. (B) The quality of AAV9-OCT4 was measured via RT-PCR and lane 7 is the representative band for the product of AAV9-OCT4.

*adeno-associated virus serotype 9, AAV9; octamer-binding transcription factor 4, OCT4; reverse transcription polymerase chain reaction, RT-PCR; viral genome, VG

3. Lateral ventricular injection of adeno-associated virus

At 4 weeks of age, the mice were anesthetized with ketamine (100mg/kg; Huons, Gyeonggi-do, Korea) and xylazine (10mg/kg; Bayer Korea, Seoul, Korea) by intraperitoneal (IP) injection and were randomly assigned to either PBS, AAV9-Null control groups or the AAV9-OCT4 treatment. Using stereotaxic, as seen in Figure 1B, the mice received a lateral ventricular injection of AAV9 vector (1.0E+12 VG/ml, 1 μl per side and 0.01 μl/s infusion rate) using stereotaxic coordinates (AP +0.3mm from bregma; ML ±0.7mm from bregma; DV −2.0mm from dura) (Figure 1C). The mice recovered in a heating chamber at 37℃ after the surgical treatment. After an hour when the mice recovered, they mice were returned to standard cages.

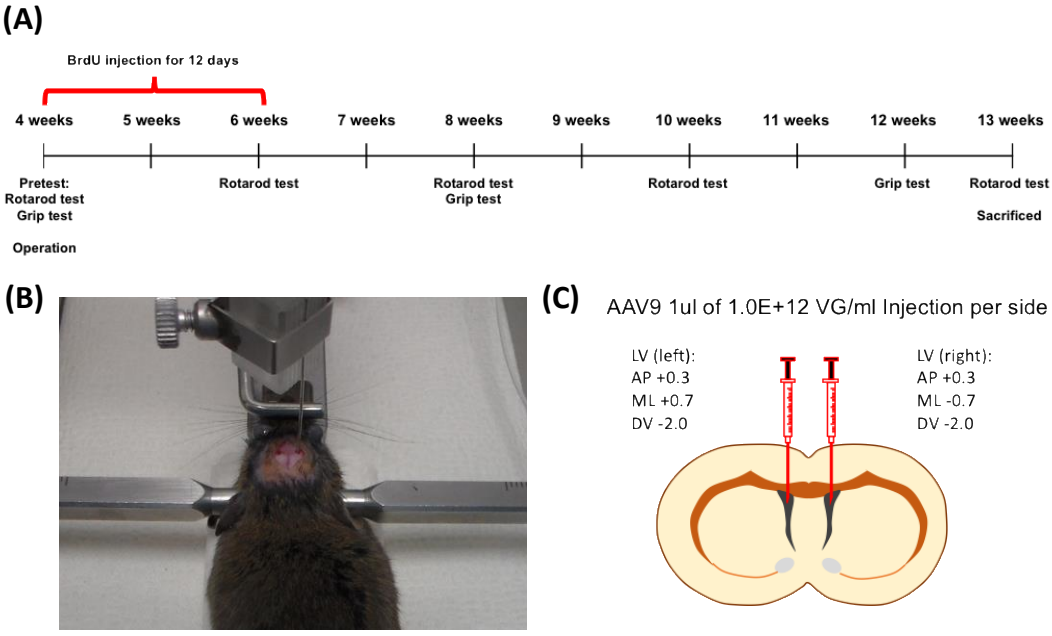

Figure 2. Study design and stereotaxic injection for the experiment (A) The schedule of behavioral tests and BrdU injection are presented in the timeline. (B) A picture showed the stereotaxic injection for the operation on the R6/2 mouse. (C) Titer and volume of the viral vector and stereotaxic coordination for lateral ventricular injection are presented.

(5-bromo-2'-deoxyuridine, BrdU; adeno associated virus serotype 9, AAV9; viral genomes, VG; lateral ventricle, LV; Anteroposterior, AP; Mediolateral, ML; Dorsoventral, DV)

4. Genotyping

Since the offspring of R6/2 mice could be either wild type or transgenic mice, pups had their genotype via genotyping PCR with their genomic DNAs.

A. Genomic DNA extraction

To extract the genomic DNA (gDNA) from the mouse, a piece of tissue from each mouse was obtained in the end of the tails about 2 mm long. The standard procedure was followed the protocol provided by the prepGEM Tissue Kit (ZyGEM, Hamilton, New Zealand). First, the pieces of the tissues were incubated in 1 μl of prepGEM, 10 μl of Buffer Gold (ZyGEM, Hamilton, New Zealand), and 89 μl of autoclaved distilled water at 75℃ for 15 minutes and then 95℃ for 5 minutes.

B. Genotyping PCR

Following the protocol provided by the Jackson Laboratory, standard PCR was performed for the genotyping through the following 10 steps using internal positive control and transgene primers (Table1): Step 1: 94℃ for 2 minutes; Step 2: 94℃ for 20 seconds; Step 3: 65℃ for 15 seconds; Step 4. 68℃ for 15 seconds and a 0.5℃ decrease per cycle; Step 5: 68℃ for 10 seconds, and repeat steps 2-4 for 10 cycles; Step 6: 94℃ for 15 seconds; Step 7: 60℃ for 15 seconds; Step 8: 72℃ for 10 seconds, and repeat steps 6-8 for 28 cycles; Step 9: 72℃ for 2 minutes, and Step 10: 10℃ holding.

Electrophoresis was performed by loading 10 ml of each PCR product on a 2%

agarose gel (Medicago, Quebec, Canada), and primers on Table 1 were used for the polymerase chain reaction (PCR). The internal positive control was 324 base pair (bp) and transgenic band was 170 bp.

Table 1. The sequence of primers used for the genotyping PCR

Primer type	Forward (5'→3')	Reverse (5'→3')	Size (bp)
Internal Positive Control	CTAGGCCACAGAATTGAAAGATCT	GTAGGTGGAAATTCTAGCATCATCC	324
Transgene	TGGAAGGACTTGAGGGACTC	CCGCTCAGGTTCTGCTTTTA	170

(base pair, bp)

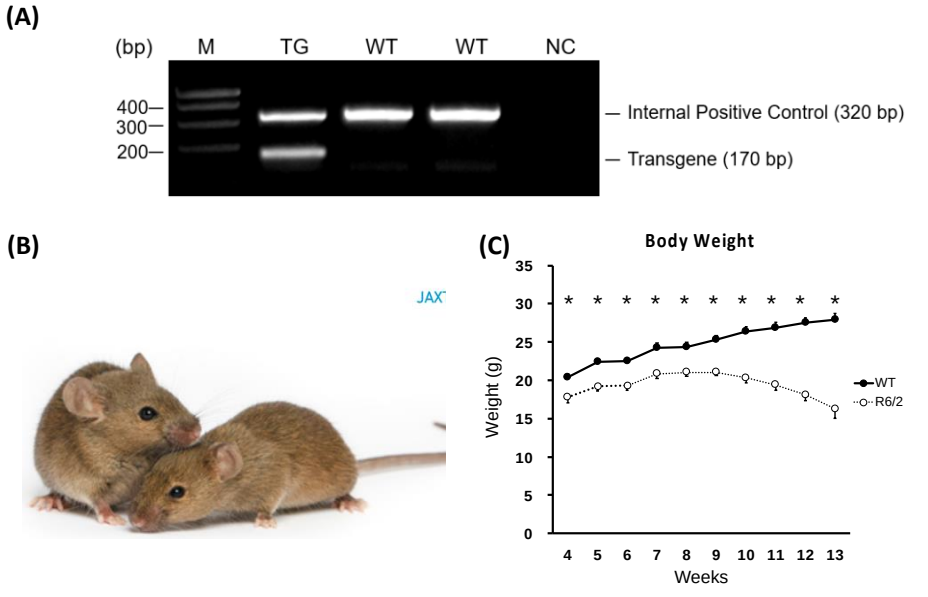

Figure 3. Genotyping and original characteristics of the R6/2 mouse model

(A) The result of genotyping that showed internal positive control on 324 bp, and transgene on 170 bp. (B) An image of R6/2 model mice from Jackson Laboratory. (C) Different characteristics between wild type normal mice and R6/2 are shown in body weight.

(* $p < 0.5$; marker, M; transgene, TG; wild type, WT; negative control, NC; base pair, bp)

5. Behavioral testsRotarod test

A rotarod test was used to assess motor coordination and locomotor function. All animals received a pretreatment performance evaluation at 4, 6, 8, 10, and 13 weeks of age. For this assessment, mice were placed on a rotarod treadmill (catalog number 47600, Ugo Basile, Comerio, Italy), and the latency to fall, which is the length of time the animals remained on the rolling rod, was measured. Rotarod tests were then performed at an average of 2-week intervals until 13 weeks after the treatment. Using an accelerating speed (4-40 rpm) and constant speed (16 rpm), the latency period when the mice fell from the rod was measured twice for each test, and an individual test was terminated at a maximum latency of 300 seconds. To avoid and reduce any stress related to the test as much as possible, the test was conducted softly.[33]

B. Grip strength test

A grip strength test was performed using the SDI Grip Strength System (San Diego Instruments Inc., San Diego, CA, USA), which includes a push–pull strain gauge. A 2-mm-diameter triangular piece of metal wire was used as the grip bar. Each animal was held near the base of its tail by a researcher and allowed to approach the bar until it was able to grip it with its forepaw. Peak force was automatically recorded in gram-force by the apparatus. The average of peak forces from the three trials was used for final data analysis. The data of the grip strength test were normalized to body weight and expressed as [KGF/kg].[34]

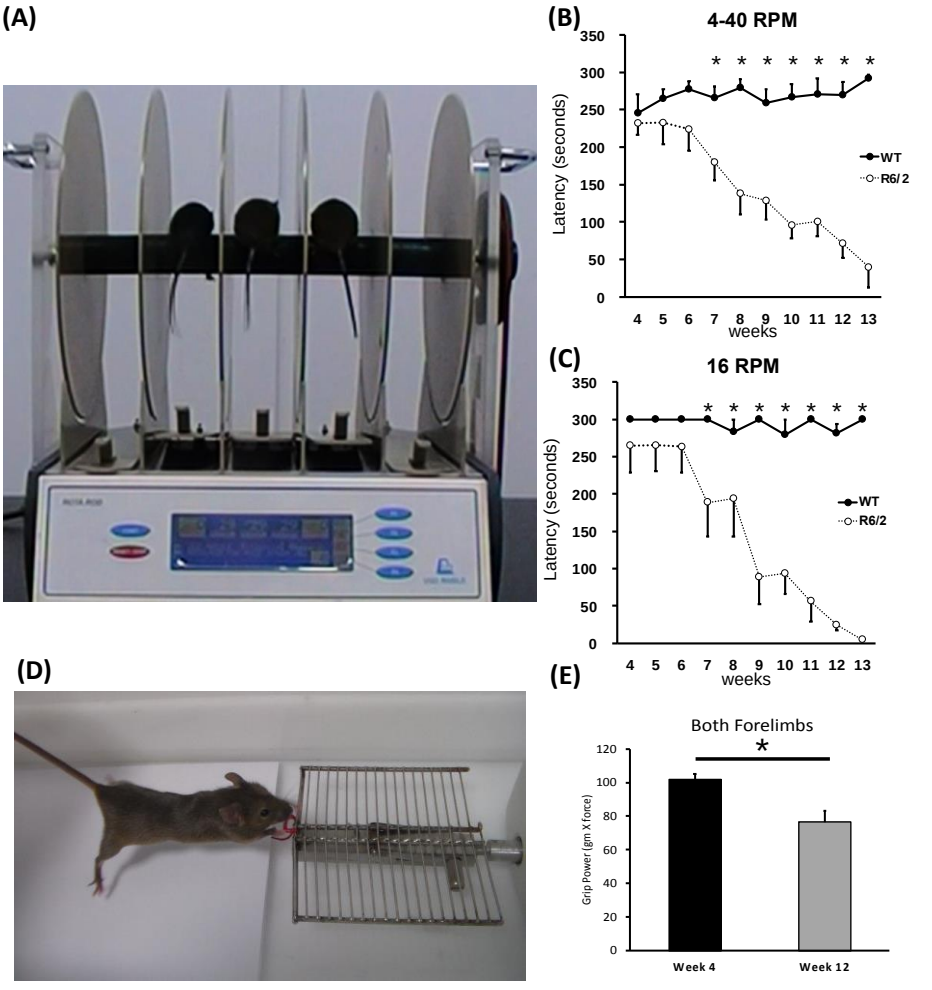

Figure 4. Rotarod and grip strength tests in WT and R6/2 (A) Three R6/2 mice are on the rotarod to evaluate the latency at a certain speed. (B) The R6/2 mouse showed a motor defect at 4-40 RPM compared to WT. (C) The R6/2 mouse showed a motor defect at 16 RPM compared to WT. (D) A grip strength test was performed for both forelimbs to evaluate the grip strength of forepaws. (E) The R6/2 mouse showed a motor defect at the terminal stage of week 12 compared to the pre-pathogenic phase of week 4 in the grip strength.
(* $p < 0.5$; wild type, WT)

6. RNA Preparation

Total RNA was extracted from both the frontal cortex and the striatum using Trizol (Invitrogen Life Technologies, Carlsbad, CA, USA). After deoxyribonuclease (DNase) digestion and clean-up procedures, the RNA samples were quantified, aliquoted, and stored at -80℃ until further use. The RNA purity was evaluated by the A260:A280 ratio and analyzed with an Agilent 2100 Bioanalyzer (Agilent Technologies, Palo Alto, CA, USA).

7. Quantitative real-time reverse transcription polymerase chain reaction (qRT-PCR)

One microgram of purified total RNA was used as a template to generate the cDNA using a ReverTra Ace qPCR TR master mix with gDNA remover (TOYOBO). The standard protocol for the qRT-PCR with SYBR Green was provided from Roche Applied Science. A total volume of 20 μl master mix with 2 μl of cDNA was used in the following reaction. The qRT-PCR was performed in triplicate on a LightCycler 480 (Roche Applied Science, Mannheim, Germany) using the LightCycler 480 SYBR Green master mix (Roche Applied Science). The thermocycler conditions were as follows: amplifications were performed starting with a 300-second template preincubation step at 95°C, followed by 40 cycles of 95°C for 5 seconds, 60°C for 2 seconds, and 95°C for 15 seconds. The melting curve analysis began at 95°C for 15 seconds, followed by 1 minute at 60°C. The specificity of the amplification product was confirmed by an examination of the melting curve, which showed a distinct single sharp peak with

the expected melting temperature (Tm) for all samples. A distinct single peak indicated that a single DNA sequence was amplified during qRT-PCR. Glyceraldehyde 3-phosphate dehydrogenase was used as an internal control. The expression of each gene of interest was obtained using the $2^{-\Delta\Delta Ct}$ method.

Table 2. The sequence of primers used for the qRT- PCR

Target Gene	Species	Forward (5'→3')	Reverse (5'→3')	Size (bp)
PDGFRa	mouse	GGAGACTCAAGTAACCTTGCAC	TCAGTTCTGACGTTGCTTTCAA	179
WNT3	mouse	TAAAGTGTAAATGCCACGGGTT	CGGAGGCACTGTCGTACTTG	117
MYRF	mouse	TCTGGGCCTCCCATCAAAG	CGGGGTTATGGTGCGTAGAAG	167
GNDF	mouse	GCCGGACGGGACTCTAAGAT	CGTCATCAAACTGGTCAGGATAA	208
GAPDH	mouse	CATCACTGCCACCCAGAAGACTG	ATGCCAGTGAGCTTCCCGTTCAG	180

(base pair, bp)

8. Immunohistochemistry

Animals were euthanized and perfused with 4% paraformaldehyde. Harvested brain tissues were cryosectioned at a slice thickness of 16 mm along the sagittal plane, and immunohistochemistry staining was performed on 4 sections over a range of over 128 mm. The tissue sections were stained with one or two following primary antibodies: 5-bromo-2'-deoxyuridine (BrdU, 1:200; Abcam, Cambridge, UK), neuron-specific class III beta-tubulin (Tuj-1, 1:400; Covance, Princeton, NJ, USA), glial fibrillary acidic protein (GFAP, 1:400; Abcam), Nestin (1:400; Abcam), neural/glial antigen 2 (NG2, 1:200, Abcam), myelin basic protein (MBP, 1:400, Abcam). The secondary antibodies such as Alexa Fluor 488 goat anti-Rat (1:400; Invitrogen), Alexa Fluor 568 goat anti-Rabbit (1:400; Invitrogen), and Alexa Fluor 594 goat anti-Mouse (1:400; Invitrogen) were used and the slide glass was mounted with fluorescent mounting medium containing 4′,6-diamidino-2-phenylindole (Vectorshield, Vector, Burlingame, CA, USA). The stained sections were analyzed using confocal microscopy (LSM780; Zeiss, Gottingen, Germany) and the MetaMorph Imaging System (Molecular Device, Sunnyvale, CA, USA).

9. Statistical analysis

All data were expressed as means ± standard error of mean (SEM). The variables between groups were analyzed using one-way analysis of variance (ANOVA) followed by a post-hoc Bonferroni and/or LSD comparison using the SPSS statistics (IBM corporation, Armonk, NY, USA; version 23.0). A P-value < 0.05

was considered to be statistically significant.

III. RESULTS

1. Behavioral tests

To evaluate the behavioral functions and validate the motor defect before and after the progress of HD, rotarod and grip strength tests were performed according to the following schedules (Figure 2A).

A. Rotarod test

During the rotarod assessment, the AAV9-OCT4 group showed significant differences between both the PBS and the AAV9-Null control groups at both accelerating and constant speed. In post treatment week 9 of the accelerating speed test, the AAV9-OCT4 group showed significantly better performance compared to both the PBS and the AAV9-Null groups (n=5-7 per group, p=0.049 and 0.020, respectively, Figure 5A). In post treatment week 6 of the constant speed, 16 RPM test, the AAV9-OCT4 group showed significantly better performance compared to both the PBS and the AAV9-Null groups (n=5-7 per group, p=0.005 and 0.048, respectively, Figure 5B). Moreover, in post treatment week 9—the terminal phase of the HD—the AAV9-OCT4 group showed greater improvement in terms of motor performance compared to both the PBS and the AAV9-Null (p=0.038 and 0.024, respectively, Figure 5B).

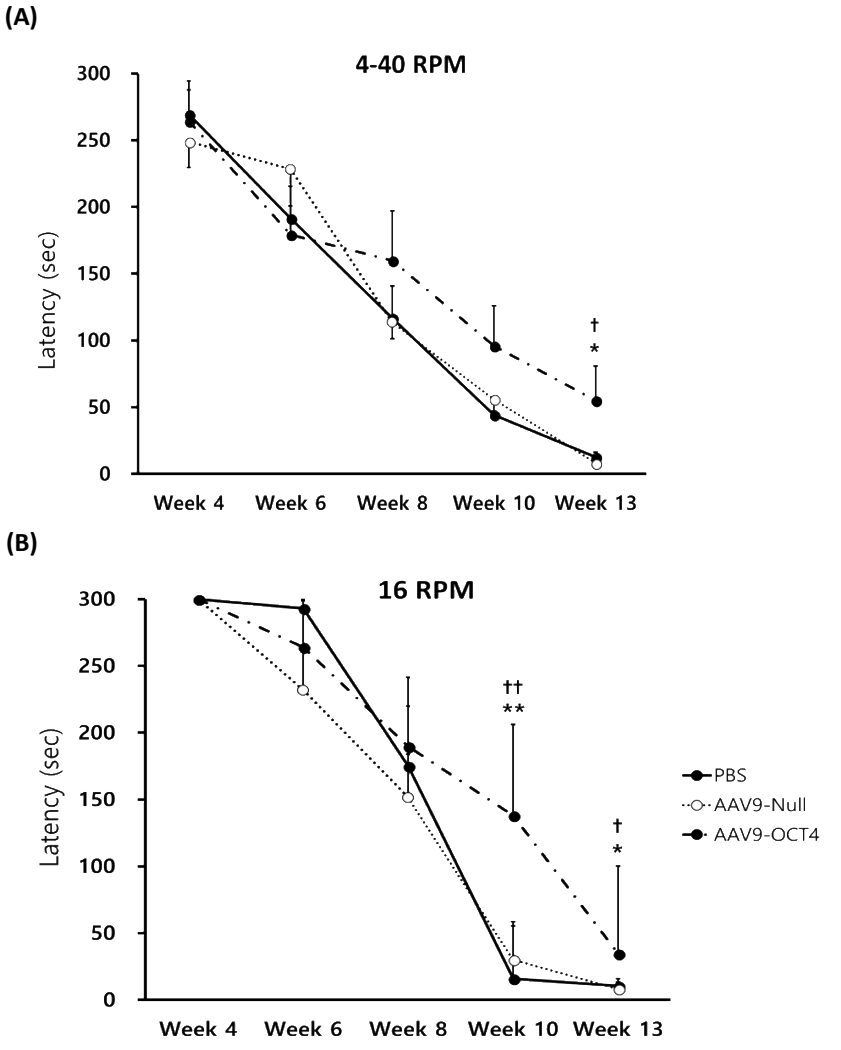

Figure 5. Rotarod test (A) The result of the rotarod test at 4-40 RPM. In week 13, the AAV9-OCT4 group showed statistical differences compared to the control groups. (B) The result of the rotarod test at 16 RPM. In both weeks 10 and 13, the AAV9-OCT4 group showed statistical differences compare to the control groups.

(n = 5-7 per group; *$p < 0.05$, **$p < 0.01$, one-way analysis of variance followed by a post-hoc LSD or Bonferroni comparison). In all panels, mean ± SEM.

B. Grip strength test

During the grip strength test the AAV9-OCT4 group showed significantly higher grip force than both the PBS and the AAV9-Null control groups at both weeks 8 and 12. During the week of treatment, the 3 groups did not show statically any differences between the groups. During post-treatment week 4, when the pathogenic symptoms began to be shown, the grip strength of the forelimbs was gradually decreased. Since post-treatment week 4, the AAV9-OCT4 group showed a significantly higher force compared to both the PBS and the AAV9-Null groups (n=5-7 per group, p=0.003 and 0.008, respectively, Figure 6). Moreover, in post-treatment week 8, the AAV9-OCT4 group showed a significantly better performance compared to both the PBS and the AAV9-Null groups (n=5-7 per group, p=0.041 and 0.032, respectively, Figure 6).

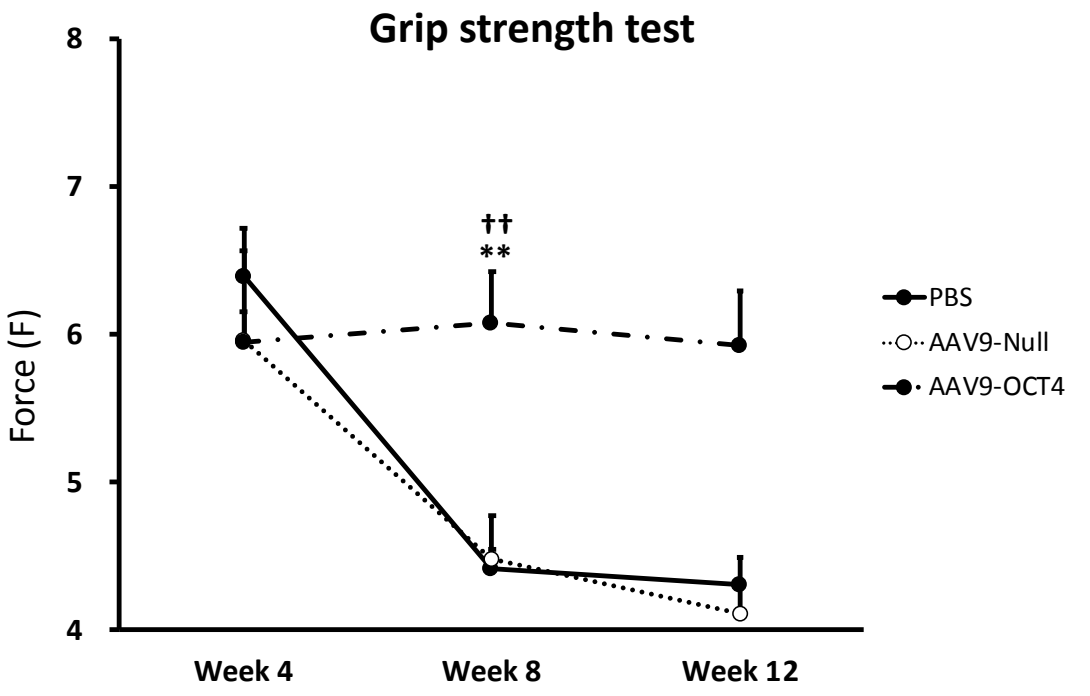

Figure 6. Grip strength test The result of grip strength test on showed motor defects since week 8; the AAV9-OCT4 group showed statistical differences compared to the two control groups.

(*$p < 0.05$, **$p < 0.01$, one-way analysis of variance followed by a post-hoc LSD or Bonferroni comparison). In all panels, mean ± SEM.

2. Quantitative real-time reverse transcription polymerase chain reaction with candidate genes selected by GeneMANIA

For the schematic study, the GeneMANIA (http://www.genemania.org) prediction server: *biological network integration for gene prioritization and predicting gene function* was used to determine and predict the relationship and functions between genes that related to OCT4 (Figure 7). Since the report showed the relationship between OCT4 and both platelet- derived growth factor receptor alpha (PDGFRa), Wnt family member 3 (WNT3) and Achaete-scute homolog 1 (ASCL1), quantification via qRT-PCR was performed on both the frontal cortex and the striatum. On the frontal cortex, expression of PDGFRa showed statistical differences between the AAV9-OCT4 and both the PBS and the AAV9-Null group (n=4-6 per group, p=0.005 and 0.004, respectively, Figure 8A), and expression of WNT3 showed statistical differences between the AAV9-OCT4 and both the PBS and the AAV9-Null group (n=4-6 per group, p=0.005 and 0.004, respectively, Figure 8B); however, the RNA expression of ASCL1 did not show any differences between the groups (n=4-6 per group, Figure 8C). On the other hand, on the striatum, the expression of PDGFRa showed statistical differences between the AAV9-OCT4 and both the PBS and the AAV9-Null group (n=4-6 per group, p=0.033 and 0.047, respectively, Figure 8D), and the expression of WNT3 showed statistical differences between the AAV9-OCT4 and both the PBS and the AAV9-Null group (n=4-6 per group, p=0.005 and 0.004, respectively, Figure 8E); however, the RNA expression of ASCL1 did show any

differences between the groups (n=4-6 per group, Figure 8F).

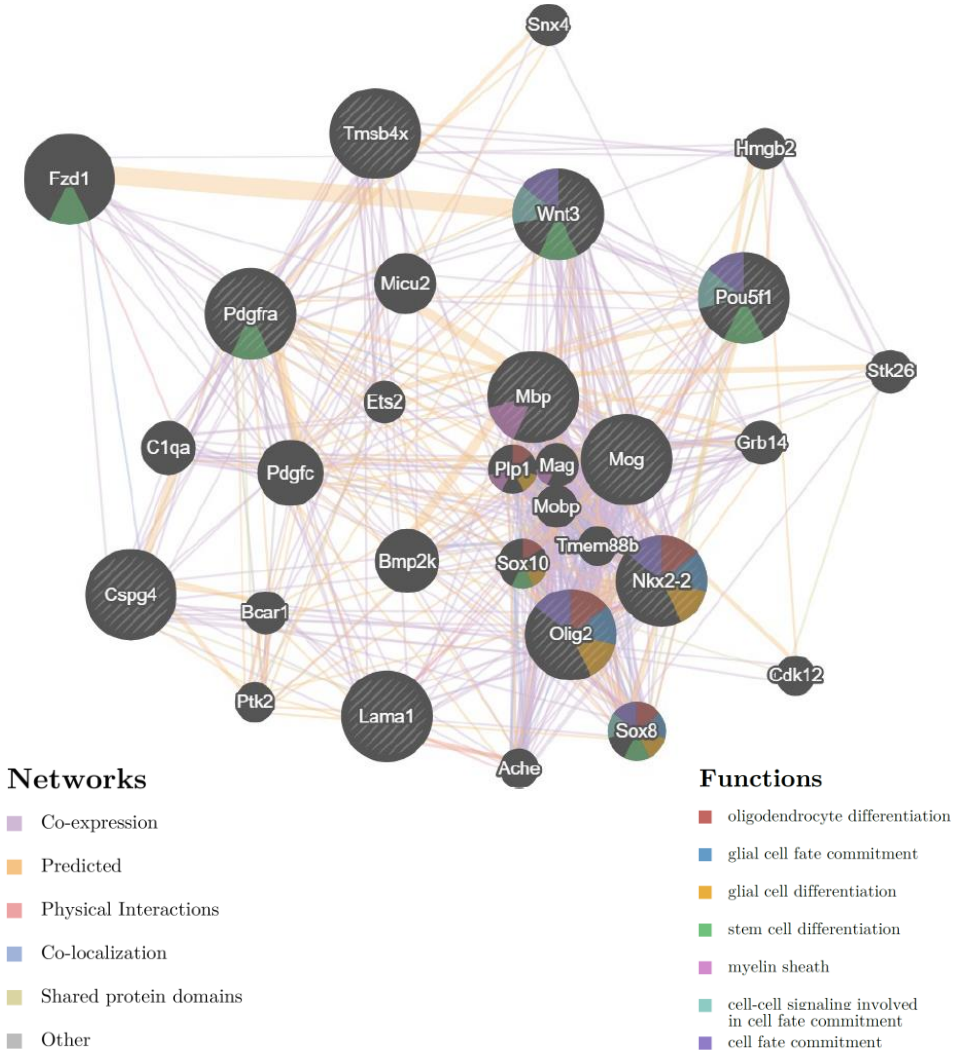

Figure 7. Gene MANIA report According to previous researches, some genes have been elucidated their relationships and functions.

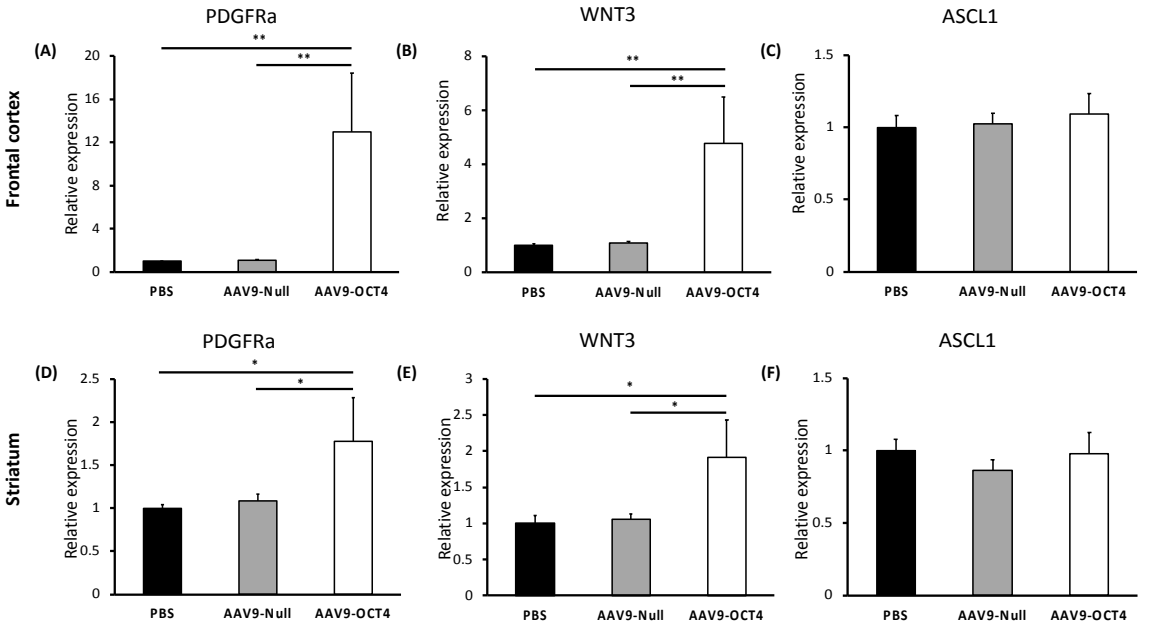

Figure 8. Quantifications of oligodendrogenesis relative RNA expression in the frontal cortex and the striatum via qRT-PCR (A) Relative RNA expression of PDGFRa on the frontal cortex. (B) Relative RNA expression of WNT3 on the frontal cortex. (C) Relative RNA expression of ASCL1 on the frontal cortex. (D) Relative RNA expression of PDGFRa on striatum (E) Relative RNA expression of WNT3 on striatum. (F) Relative RNA expression of ASCL1 on the striatum.

(*$p < 0.05$, **$p < 0.01$, one-way analysis of variance followed by a post-hoc LSD or Bonferroni comparison). In all panels, mean ± SEM.

3. Immunohistochemistry

Since the BrdU can track the newly proliferated cells via immunohistochemistry (IHC), the fate of neuronal cells was validated by the counting of Nestin or Tuj-1 with BrdU. Also, newly proliferated cells which have the possibility of differentiated to oligodendrocyte were counted as NG2 or GFAP with BrdU double positive cells. In Figure 9A, Nestin+BrdU+ positive cells are significantly higher in the AAV9-OCT4 group than in the other two control groups in the subventricular zone (n=3-4 per group, p=0.006 and 0.006, respectively, Figure 9A); representative images are shown in Figure 9C. In Figure 9B, Tuj-1+BrdU+ cells are not significantly higher in the AAV9-OCT4 group than in the other two control groups in the subventricular zone (n=3-4 per group, Figure 9B); representative images are shown in Figure 9D. In Figure 10A, NG2+BrdU+ cells are significantly higher in the AAV9-OCT4 group than in the other two control groups in the subventricular zone (n=3-4 per group, p=0.027 and 0.015, respectively, Figure 10A); representative images are shown in Figure 10C. In Figure 10B, GFAP+BrdU+ cells not significantly higher in the AAV9-OCT4 group than in the other two control groups in the subventricular zone (n=3-4 per group, Figure 10B); representative images are shown in Figure 9D.

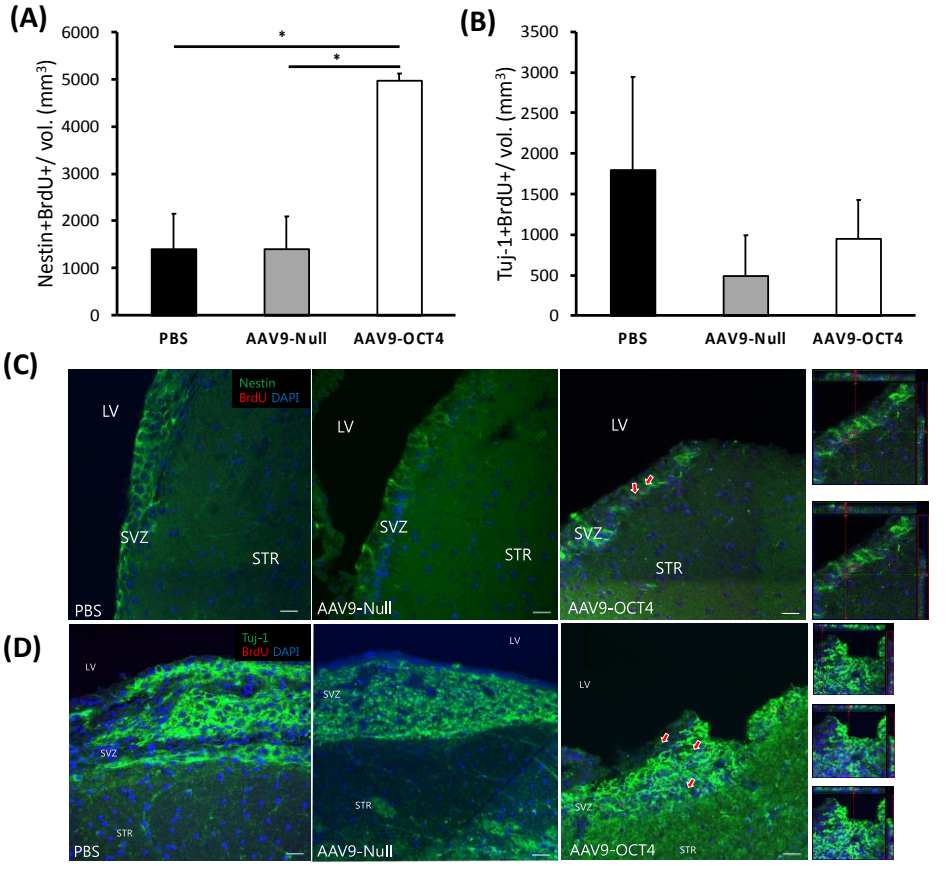

Figure 9. Nestin or Tuj-1 with BrdU double positive cells in the subventricular zone (A) Nestin+BrdU+ cells are counted and the compared between the three groups—PBS, AAV9-Null, and AAV9-OCT4. (B) Tuj-1+BrdU+ cells are counted and compared between the three groups—PBS, AAV9-Null, and AAV9-OCT4. (C) The representative images of Nestin+BrdU+ cell in the PBS, AAV9-Null and the AAV9-OCT4 groups. (D) The representative images of Tuj-1+BrdU+ cell in the PBS, AAV9-Null and the AAV9-OCT4 groups.

(*$p < 0.05$, **$p < 0.01$, one-way analysis of variance followed by a post-hoc LSD or Bonferroni comparison). In all panels, mean ± SEM.

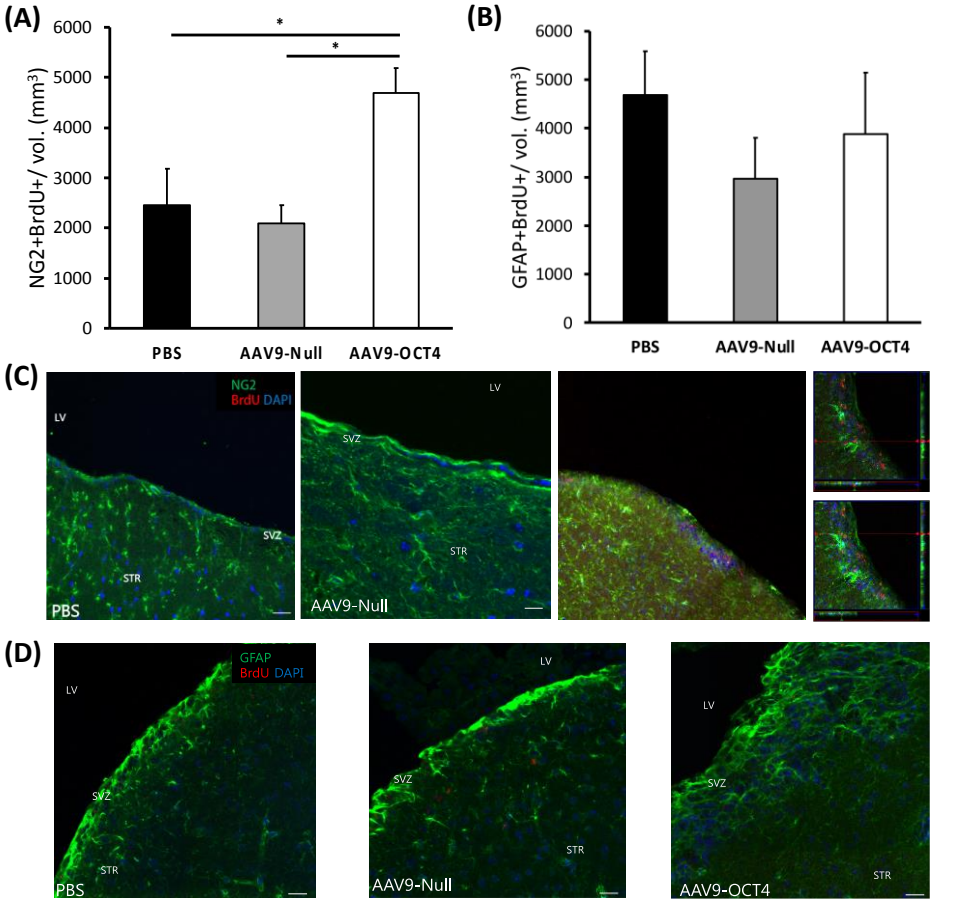

Figure 10. NG2 or GFAP with BrdU double positive cells in the subventricular zone (A) NG2+BrdU+ cells are counted and compared between the three groups—PBS, AAV9-Null, and AAV9-OCT4. (B) GFAP+BrdU+ cells are counted and compared between the three groups—PBS, AAV9-Null, and AAV9-OCT4. (C) The representative images of NG2+BrdU+ cells in the PBS, AAV9-Null and the AAV9-OCT4 groups. (D) The representative images of GFAP+ and/or BrdU+ cells in the PBS, AAV9-Null and the AAV9-OCT4 groups. (*$p < 0.05$, **$p < 0.01$, one-way analysis of variance followed by a post-hoc LSD or Bonferroni comparison). In all panels, mean ± SEM.

4. Quantitative real-time reverse transcription polymerase chain reaction of myelin regulatory factor genes

Myelin regulatory factor (MYRF) was validated in both the frontal cortex and the striatum via qRT-PCR. The RNA level of MYRF expression in the frontal cortex showed significant differences in the AAV9-OCT4 compared to the control groups (*p=.012; 0.36, respectively, Figure 11C)

5. Western blot analysis

Myelin basic protein (MBP) was validated in the protein level to confirm dysmyelination in both the frontal cortex and the striatum via western blot. On Figure 12A showed the MBP (19 and 26 kilo Dalton) in the frontal cortex. The expression of MBP in the control groups—PBS and AAV9-Null—was significantly lower than in the AAV9-OCT4 group (*p=.012 and 0.36, respectively, Figure 12C). Representative IHC images on the frontal cortex were presented in Figure 11E. Furthermore, Figure 12B showed the protein bands in each group. In the striatum, control groups showed a decreasing tendency compared to the AAV9-OCT4 group (Figure 12D). Representative IHC images on the striatum were presented in Figure 12F.

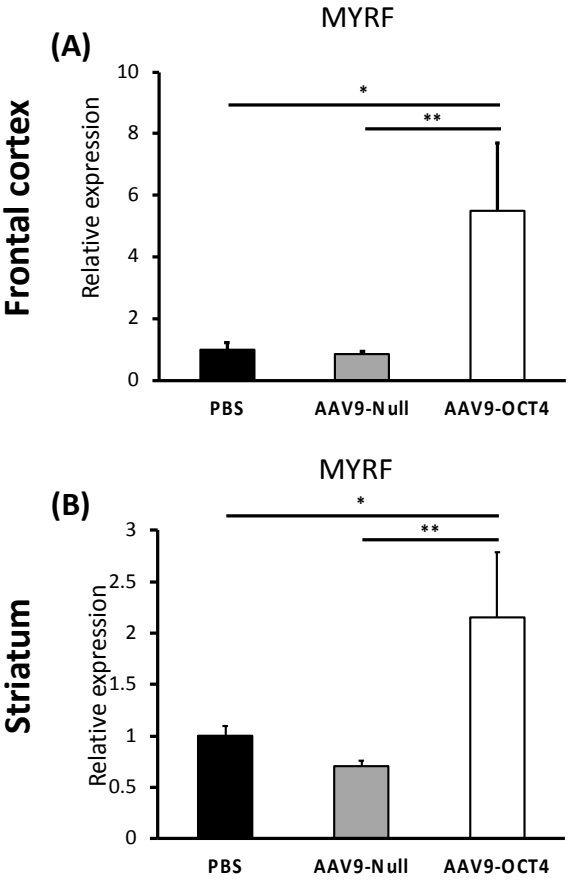

Figure 11. Quantifications of myelin regulatory factor RNA expression in the frontal cortex and the striatum via qRT-PCR. (A) Relative RNA expression of MYRF on the frontal cortex. (B) Relative RNA expression of GDNF on the striatum.

(*$p < 0.05$, **$p < 0.01$, one-way analysis of variance followed by a post-hoc LSD or Bonferroni comparison). In all panels, mean ± SEM.

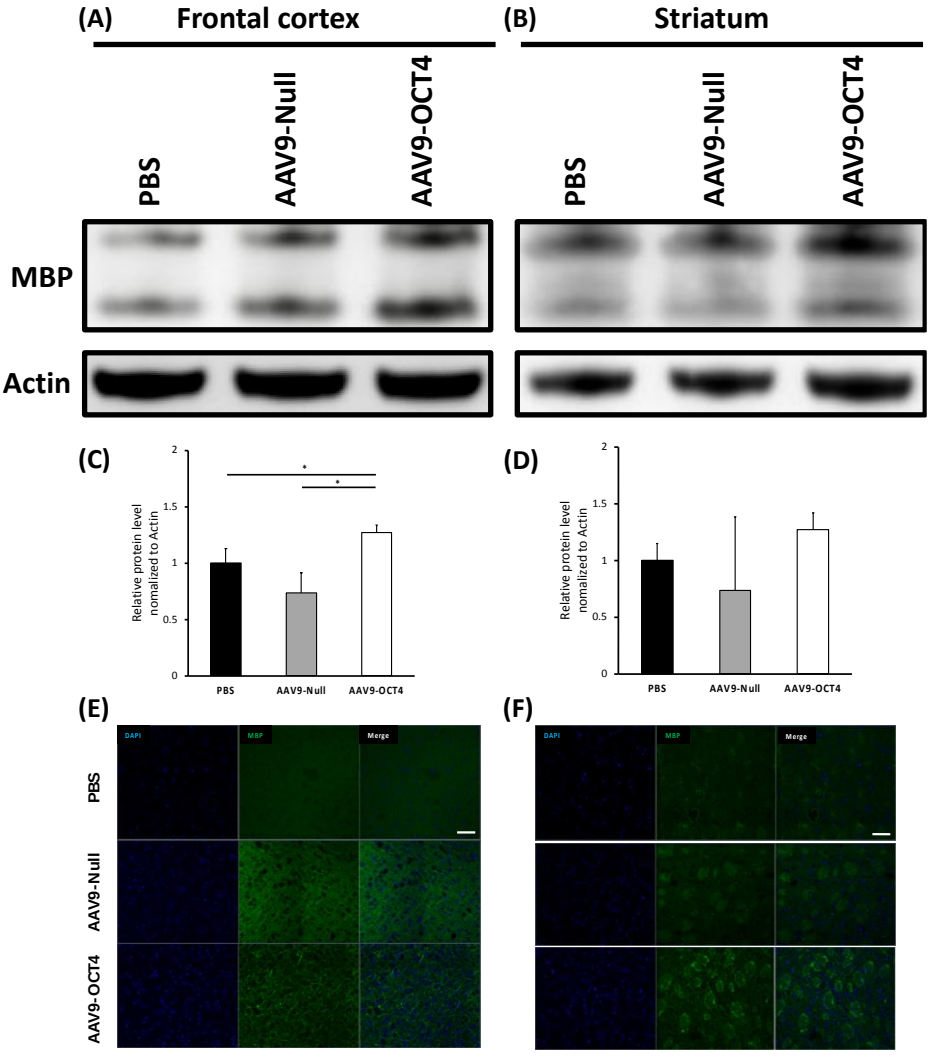

Figure 12. Western blot and immunohistochemistry result of MBP in the frontal cortex and the striatum (A) Western blot bands for each group in the frontal cortex. (B) Western blot bands for each group in the striatum. (C) Graph of western blot analysis for MBP in the frontal cortex. (D) Graph of western blot analysis for MBP in the striatum. (E) Images of IHC for MBP in the frontal cortex (F) Images of IHC for MBP in the striatum

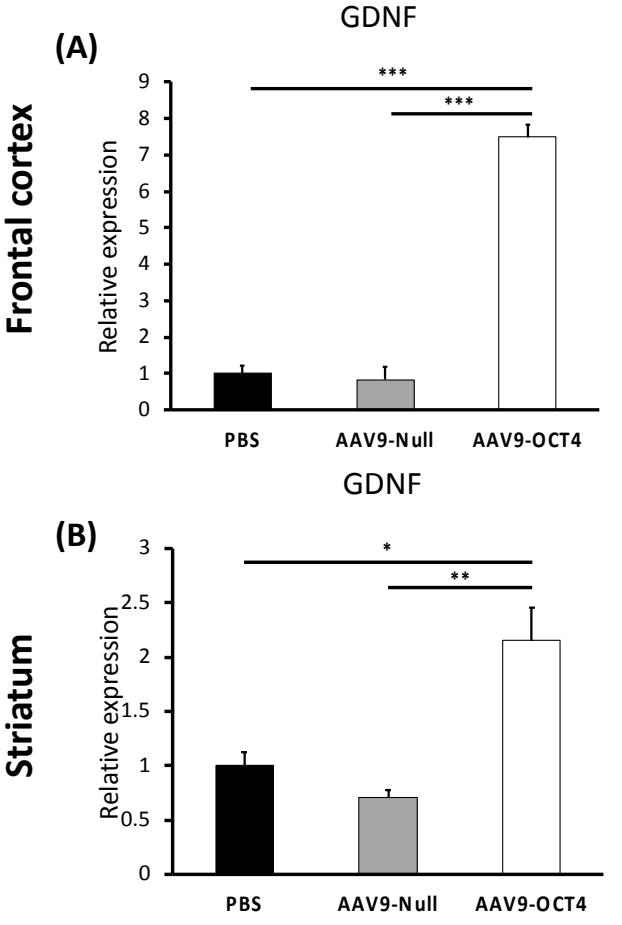

Figure 13. Figure 13. Quantifications of expression of oligodendrocyte secreted RNA in the frontal cortex and the striatum via qRT-PCR (A) Relative RNA expression of GDNF in the frontal cortex. (B) Relative RNA expression of GDNF in the striatum.

(*$p < 0.05$, **$p < 0.01$, one-way analysis of variance followed by a post-hoc LSD or Bonferroni comparison). In all panels, mean ± SEM

IV. DISCUSSION

This study treated R6/2 mice with OCT4, and the result was that the treatment group was improved in terms of their behavioral functions. White matter abnormalities have been reported in premanifest Huntington's disease (HD) subjects before the significant striatal neuronal loss; however, the pathological study and understanding of mechanism of these abnormalities are not clearly elucidated.[6] Furthermore, recent studies have been reported that white matter is associated with motor and cognitive functions, so white matter atrophy in HD causes motor and emotional defects.[35,36] Current data demonstrating white matter abnormalities in PGC1 knock-out (KO) mice provoked us to examine the role of PGC1 in CNS myelination and its relevance to HD pathogenesis.[37] Decreased expression of MBP and deficient myelination were found postnatally and in the adult R6/2 mouse model of HD.[37]

Since the behavioral data of this study in rotarod and grip strength showed the differences between the control groups and the OCT4 overexpression group, OCT4 may be the main factor for these differences. Since it is possible for AAV9 to pass through blood brain barrier[38,39], AAV9 based vectors injected in the lateral ventricle were able to influence in the subventricular zone. While OCT4 overexpressed in the subventricular zone and oligodendrocyte progenitor cells increased, PDGFRa secreted by oligodendrocyte progenitor cells would be increased.[32] Also, WNT3 was co-expressed with OCT4.[40,41] The result of the validation of qRT-PCR showed that PDGFRa and WNT3, which have very

important roles to play in maturation and proliferation in oligodendrocyte[42,43], were increased in the AAV9-OCT4 group. Since the WNT3 was upregulated, WNT3 plays a crucial role in promoting oligodendrocyte specification in the adult subventricular zone.[44] Both these genes help stem cells in the subventricular zone to turn into oligodendrocyte progenitor cells. Through immunohistochemistry, this study found that Nestin and BrdU double positive cells increased, and at the same time, NG2 and BrdU double positive cells increased in the treatment group. These results show that the OCT4 induced proliferation in the subventricular zone.

While oligodendrocyte progenitor cells were induced, those cells upregulated MYRF, so oligodendrocyte progenitor cells were induced and became fully differentiated oligodendrocyte with myelin.[45] Since mutant huntingtin is directly involved in downregulation of MYRF and occurred demylination[45], the result of upregulated MYRF by OCT4 showed the possibility of remyelination in the brain. The protein level of MBP was validated via western blotting, and the result showed the remyelination in the treatment group compared to the control groups. Production of myelin proteins in mature oligodendrocytes is important for the preservation of myelin in adult brains.[45] Mutant huntingtin did not reduce the Olig2 but only affected in the MYRF that is expressed only in post mitotic oligodendrocyte.[45] Therefore, improving the function of mature oligodendrocyte will alleviate the symptoms of HD. Moreover, when the mature oligodendrocyte increased, a neuroprotective effect factor such as GDNF secreted from

oligodendrocyte[46-49] could be increased at the same time.

As a consequence of the injection of OCT4 in vivo, PDGFRa and WNT3 were stimulated and upregulated. These two upregulated genes induce differentiation of precursor cells to oligodendrocyte. The increase of postmitotic oligodendrocytes increased MYRF, so remyelination was induced. Additionally, the neuroprotective functions of GDNF which secreted from oligodendrocyte could be a benefit of the neuroprotective effects on GABAergic neurons in the striatum and alleviate the disease all of which have been reported to recover of behavioral functions.

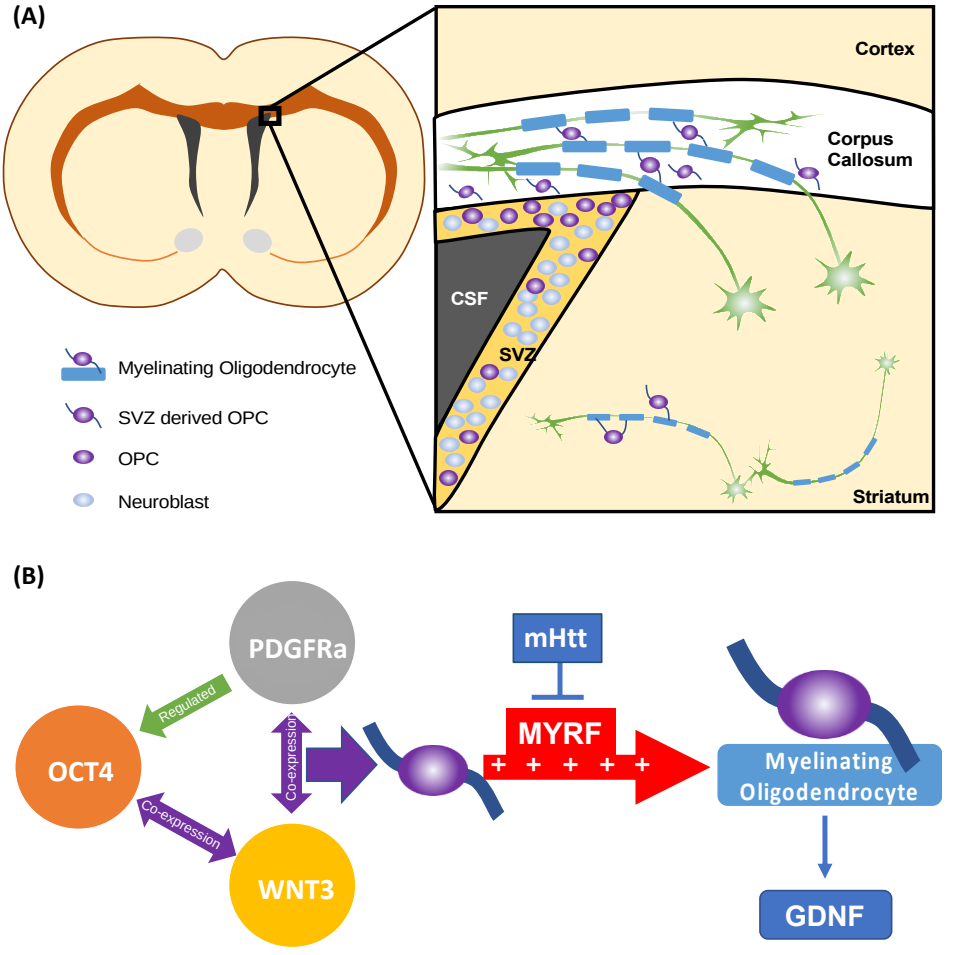

Figure 14. Diagram for conclusion (A) A picture of the subventricular zone and the location of OPC, neuroblast, oligodendrocyte cells in the brain. (B) OCT4 and PDGFRa and WNT3 were closely related and interactive their regulation. As a result of upregulation of WNT3 and PDGFRa, defected MYRF by mHtt might recover the transcription and upregulated, recovered MYRF might induce oligodendrocyte with myelin.
(oligodendrocyte progenitor cell, OPC; Platelet derived growth factor receptor, alpha polypeptide, PDGFRa; Wingless-type MMTV integration site family, member 3, WNT3; myelin regulatory factor, MYRF)

V. CONCLUSION

The findings of this study suggest that improving the function of mature oligodendrocytes by OCT4 should at least be beneficial in HD and perhaps other age-related neurodegenerative diseases that involve the dysfunction of mature oligodendrocytes and associated axonal dysfunction as well. Thus, OCT4 could be the important therapeutic factor for HD.

REFERENCES

1. Precious SV, Rosser AE. Producing striatal phenotypes for transplantation in Huntington's disease. Experimental Biology and Medicine 2012;237:343-51.
2. Cicchetti F, Soulet D, Freeman TB. Neuronal degeneration in striatal transplants and Huntington's disease: potential mechanisms and clinical implications. Brain 2011;134:641-52.
3. Ruocco HH, Lopes-Cendes I, Li LM, Santos-Silva M, Cendes F. Striatal and extrastriatal atrophy in Huntington's disease and its relationship with length of the CAG repeat. Braz J Med Biol Res 2006;39:1129-36.
4. Zuccato C, Valenza M, Cattaneo E. Molecular mechanisms and potential therapeutical targets in Huntington's disease. Physiol Rev 2010;90:905-81.
5. Rosas HD, Lee SY, Bender AC, Zaleta AK, Vangel M, Yu P, et al. Altered white matter microstructure in the corpus callosum in Huntington's disease: implications for cortical "disconnection". Neuroimage 2010;49:2995-3004.
6. Jin J, Peng Q, Hou Z, Jiang M, Wang X, Langseth AJ, et al. Early white matter abnormalities, progressive brain pathology and motor deficits in a novel knock-in mouse model of Huntington's disease. Hum Mol Genet 2015;24:2508-27.
7. Fennema-Notestine C, Archibald SL, Jacobson MW, Corey-Bloom J, Paulsen JS, Peavy GM, et al. In vivo evidence of cerebellar atrophy and cerebral white matter loss in Huntington disease. Neurology 2004;63:989-95.
8. Gomez-Tortosa E, MacDonald ME, Friend JC, Taylor SA, Weiler LJ, Cupples LA, et al. Quantitative neuropathological changes in presymptomatic Huntington's disease. Ann Neurol 2001;49:29-34.
9. Myers RH, Vonsattel JP, Paskevich PA, Kiely DK, Stevens TJ, Cupples LA, et al. Decreased neuronal and increased oligodendroglial densities in Huntington's disease caudate nucleus. J Neuropathol Exp Neurol 1991;50:729-42.
10. Nopoulos PC, Aylward EH, Ross CA, Mills JA, Langbehn DR, Johnson HJ, et al. Smaller intracranial volume in prodromal Huntington's disease: evidence for abnormal neurodevelopment. Brain 2011;134:137-42.
11. Paulsen JS, Langbehn DR, Stout JC, Aylward E, Ross CA, Nance M, et al. Detection of Huntington's disease decades before diagnosis: the Predict-HD study. J Neurol Neurosurg Psychiatry 2008;79:874-80.
12. Reading SA, Yassa MA, Bakker A, Dziorny AC, Gourley LM, Yallapragada V, et al. Regional white matter change in pre-symptomatic Huntington's disease: a diffusion tensor imaging study. Psychiatry Res 2005;140:55-62.
13. Tabrizi SJ, Langbehn DR, Leavitt BR, Roos RA, Durr A, Craufurd D, et al. Biological and clinical manifestations of Huntington's disease in the longitudinal TRACK-HD study: cross-sectional analysis of baseline data. Lancet Neurol 2009;8:791-801.
14. Weaver KE, Richards TL, Liang O, Laurino MY, Samii A, Aylward EH. Longitudinal diffusion tensor imaging in Huntington's Disease. Exp Neurol 2009;216:525-9.
15. Aylward EH, Nopoulos PC, Ross CA, Langbehn DR, Pierson RK, Mills JA, et al. Longitudinal change in regional brain volumes in prodromal Huntington disease. Journal of Neurology, Neurosurgery & Psychiatry 2011;82:405-10.
16. Ciarmiello A, Cannella M, Lastoria S, Simonelli M, Frati L, Rubinsztein DC, et

al. Brain white-matter volume loss and glucose hypometabolism precede the clinical symptoms of Huntington's disease. Journal of Nuclear Medicine 2006;47:215-22.
17. Paulsen JS, Magnotta VA, Mikos AE, Paulson HL, Penziner E, Andreasen NC, et al. Brain structure in preclinical Huntington's disease. Biological psychiatry 2006;59:57-63.
18. Paulsen JS, Nopoulos PC, Aylward E, Ross CA, Johnson H, Magnotta VA, et al. Striatal and white matter predictors of estimated diagnosis for Huntington disease. Brain research bulletin 2010;82:201-7.
19. Thieben M, Duggins A, Good C, Gomes L, Mahant N, Richards F, et al. The distribution of structural neuropathology in pre-clinical Huntington's disease. Brain 2002;125:1815-28.
20. Beglinger LJ, Nopoulos PC, Jorge RE, Langbehn DR, Mikos AE, Moser DJ, et al. White matter volume and cognitive dysfunction in early Huntington's disease. Cognitive and Behavioral Neurology 2005;18:102-7.
21. Rosas HD, Koroshetz W, Chen Y, Skeuse C, Vangel M, Cudkowicz M, et al. Evidence for more widespread cerebral pathology in early HD An MRI-based morphometric analysis. Neurology 2003;60:1615-20.
22. Aylward EH, Li Q, Stine O, Ranen N, Sherr M, Barta P, et al. Longitudinal change in basal ganglia volume in patients with Huntington's disease. Neurology 1997;48:394-9.
23. Georgiou-Karistianis N, Scahill R, Tabrizi SJ, Squitieri F, Aylward E. Structural MRI in Huntington's disease and recommendations for its potential use in clinical trials. Neuroscience & Biobehavioral Reviews 2013;37:480-90.
24. Hobbs NZ, Henley SM, Ridgway GR, Wild EJ, Barker RA, Scahill RI, et al. The progression of regional atrophy in premanifest and early Huntington's disease: a longitudinal voxel-based morphometry study. Journal of Neurology, Neurosurgery & Psychiatry 2010;81:756-63.
25. Tabrizi SJ, Scahill RI, Durr A, Roos RA, Leavitt BR, Jones R, et al. Biological and clinical changes in premanifest and early stage Huntington's disease in the TRACK-HD study: the 12-month longitudinal analysis. The Lancet Neurology 2011;10:31-42.
26. Crawford HE, Hobbs NZ, Keogh R, Langbehn DR, Frost C, Johnson H, et al. Corpus callosal atrophy in premanifest and early Huntington's disease. Journal of Huntington's disease 2013;2:517-26.
27. Ross CA, Aylward EH, Wild EJ, Langbehn DR, Long JD, Warner JH, et al. Huntington disease: natural history, biomarkers and prospects for therapeutics. Nat Rev Neurol 2014;10:204-16.
28. Bartzokis G, Lu PH, Tishler TA, Fong SM, Oluwadara B, Finn JP, et al. Myelin breakdown and iron changes in Huntington's disease: pathogenesis and treatment implications. Neurochem Res 2007;32:1655-64.
29. Seo JH, Lee MY, Yu JH, Kim MS, Song M, Seo CH, et al. In Situ Pluripotency Factor Expression Promotes Functional Recovery From Cerebral Ischemia. Mol Ther 2016;24:1538-49.
30. Wi S, Yu JH, Kim M, Cho SR. In Vivo Expression of Reprogramming Factors Increases Hippocampal Neurogenesis and Synaptic Plasticity in Chronic Hypoxic-Ischemic Brain Injury. Neural Plast 2016;2016:2580837.
31. Kim JB, Sebastiano V, Wu G, Arauzo-Bravo MJ, Sasse P, Gentile L, et al. Oct4-

induced pluripotency in adult neural stem cells. Cell 2009;136:411-9.
32. Kim JB, Lee H, Arauzo-Bravo MJ, Hwang K, Nam D, Park MR, et al. Oct4-induced oligodendrocyte progenitor cells enhance functional recovery in spinal cord injury model. EMBO J 2015;34:2971-83.
33. Lee MY, Yu JH, Kim JY, Seo JH, Park ES, Kim CH, et al. Alteration of synaptic activity-regulating genes underlying functional improvement by long-term exposure to an enriched environment in the adult brain. Neurorehabil Neural Repair 2013;27:561-74.
34. Spurney CF, Gordish-Dressman H, Guerron AD, Sali A, Pandey GS, Rawat R, et al. Preclinical drug trials in the mdx mouse: assessment of reliable and sensitive outcome measures. Muscle Nerve 2009;39:591-602.
35. Beglinger LJ, Nopoulos PC, Jorge RE, Langbehn DR, Mikos AE, Moser DJ, et al. White matter volume and cognitive dysfunction in early Huntington's disease. Cogn Behav Neurol 2005;18:102-7.
36. Faria AV, Ratnanather JT, Tward DJ, Lee DS, van den Noort F, Wu D, et al. Linking white matter and deep gray matter alterations in premanifest Huntington disease. Neuroimage Clin 2016;11:450-60.
37. Xiang Z, Valenza M, Cui L, Leoni V, Jeong HK, Brilli E, et al. Peroxisome-proliferator-activated receptor gamma coactivator 1 alpha contributes to dysmyelination in experimental models of Huntington's disease. J Neurosci 2011;31:9544-53.
38. Gholizadeh S, Tharmalingam S, Macaldaz ME, Hampson DR. Transduction of the central nervous system after intracerebroventricular injection of adeno-associated viral vectors in neonatal and juvenile mice. Hum Gene Ther Methods 2013;24:205-13.
39. Sohn J, Orosco L, Guo F, Chung SH, Bannerman P, Mills Ko E, et al. The subventricular zone continues to generate corpus callosum and rostral migratory stream astroglia in normal adult mice. J Neurosci 2015;35:3756-63.
40. Kelly KF, Ng DY, Jayakumaran G, Wood GA, Koide H, Doble BW. beta-catenin enhances Oct-4 activity and reinforces pluripotency through a TCF-independent mechanism. Cell Stem Cell 2011;8:214-27.
41. Zhang X, Peterson KA, Liu XS, McMahon AP, Ohba S. Gene regulatory networks mediating canonical Wnt signal-directed control of pluripotency and differentiation in embryo stem cells. Stem Cells 2013;31:2667-79.
42. Lo Nigro A, de Jaime-Soguero A, Khoueiry R, Cho DS, Ferlazzo GM, Perini I, et al. PDGFRalpha(+) Cells in Embryonic Stem Cell Cultures Represent the In Vitro Equivalent of the Pre-implantation Primitive Endoderm Precursors. Stem Cell Reports 2017;8:318-33.
43. Zawadzka M, Rivers LE, Fancy SP, Zhao C, Tripathi R, Jamen F, et al. CNS-resident glial progenitor/stem cells produce Schwann cells as well as oligodendrocytes during repair of CNS demyelination. Cell Stem Cell 2010;6:578-90.
44. Ortega F, Gascon S, Masserdotti G, Deshpande A, Simon C, Fischer J, et al. Oligodendrogliogenic and neurogenic adult subependymal zone neural stem cells constitute distinct lineages and exhibit differential responsiveness to Wnt signalling. Nat Cell Biol 2013;15:602-13.
45. Huang B, Wei W, Wang G, Gaertig MA, Feng Y, Wang W, et al. Mutant huntingtin downregulates myelin regulatory factor-mediated myelin gene

expression and affects mature oligodendrocytes. Neuron 2015;85:1212-26.
46. Pineda JR, Rubio N, Akerud P, Urban N, Badimon L, Arenas E, et al. Neuroprotection by GDNF-secreting stem cells in a Huntington's disease model: optical neuroimage tracking of brain-grafted cells. Gene Ther 2007;14:118-28.
47. Sypecka J, Sarnowska A. The neuroprotective effect exerted by oligodendroglial progenitors on ischemically impaired hippocampal cells. Mol Neurobiol 2014;49:685-701.
48. Nave KA, Trapp BD. Axon-glial signaling and the glial support of axon function. Annu Rev Neurosci 2008;31:535-61.
49. Bradl M, Lassmann H. Oligodendrocytes: biology and pathology. Acta Neuropathol 2010;119:37-53.

ABSTRACT (IN KOREAN)

헌팅턴 병의 유전자 변형 마우스 모델에서 수초 감소를 완화하기 위해 OCT4로 희소 돌기 아교 세포의 수초 재생 유도

지도교수 조성래

연세대학교 대학원 의과학과

김 민 지

헌팅턴 병 (HD)은 유전자 돌연변이에 의해 발생하는 질병으로 오늘날에도 치료 방법이 없는 난치병으로 알려진 신경 퇴행성 질환이다. 최근 연구에서는 뇌백질 위축이 HD에서 초기 증상으로 밝혀지고 있다. 따라서 이 연구에서는 HD의 치료제로써 OCT4의 생체 내 과발현을 이용하여 헌팅턴에서의 수초 수축 치료에 이용하였다. 아데노 수반 바이러스 혈청 형 9 (AAV9)을 OCT4의 과잉 발현을 위한 벡터로 사용했다. R6/2 마우스의 양쪽 측면 뇌실에 PBS, AAV9-Null 또는 AAV9-OCT4를 주사했다. 그 결과, 대조군—PBS 및 AAV9-Null—및

AAV9-OCT4 군 사이에서 로터로드 및 악력 시험 등의 행동 시험에서 유의 한 개선을 보였다. RNA 발현 수준은 PDGFRα, WNT3, MYFR 및 GDNF에서 유의하게 증가하였다. 또한 Nestin+BrdU+와 NG2+BrdU+ 세포는 뇌실 하 영역의 대조군과 비교하여 AAV9-OCT4 군에서 증가하였다. 또한 MBP 단백질의 수준은 전두엽 피질에서 AAV9-OCT4에서 유의하게 증가하였다. 이러한 결과들을 종합해보면 뇌실 하부 영역에서의 재 프로그램 화 인자인 OCT4의 생체 내 과발현에 의해 희돌기교세포 전구체가 희돌기교세포로 형성이 유발된 것을 시사하고 있으며, 따라서 수초형성부진이 완화되었다. 또한 희돌기 신경 교세포에서 GDNF 분비와 같은 성장 인자는 HD의 뇌의 환경을 개선여, R6/2 마우스에서 행동 개선이 일어났다. 따라서 이 연구는 OCT4을 HD를 포함한 신경 퇴행성 질환의 치료 인자의 후보로 시사하는 바이다.

핵심되는 말 : 헌팅턴 병, 신경 퇴행성 질환, 재 프로그램 인자, OCT4, 뇌실하대, 희돌기교세포재생, 희돌기교세포, 연조직 형성 결핍

PUBLICATION LIST

1. **Kim M**, Yu JH, Seo JH, Shin YK, Wi S, Baek A, et al. Neurobehavioral Assessments in a Mouse Model of Neonatal Hypoxic-ischemic Brain Injury. J Vis Exp 2017; doi:10.3791/55838.
2. Baek A, **Kim M**, Kim SH, Cho SR, Kim HJ. Anti-inflammatory Effect of DNA Polymeric Molecules in a Cell Model of Osteoarthritis. Inflammation 2018;41:677-88.
3. Wi S, Lee JW, **Kim M**, Park CH, Cho SR. An Enriched Environment Ameliorates Oxidative Stress and Olfactory Dysfunction in Parkinson's Disease with alpha-Synucleinopathy. Cell Transplant 2018; doi:10.1177/0963689717742662.963689717742662.
4. Wi S, Yu JH, **Kim M**, Cho SR. In Vivo Expression of Reprogramming Factors Increases Hippocampal Neurogenesis and Synaptic Plasticity in Chronic Hypoxic-Ischemic Brain Injury. Neural Plast 2016;2016:2580837.
5. Kim MS, Yu JH, Lee MY, Kim AL, Jo MH, **Kim M**, et al. Differential Expression of Extracellular Matrix and Adhesion Molecules in Fetal-Origin Amniotic Epithelial Cells of Preeclamptic Pregnancy. PLoS One 2016;11:e0156038.
6. Won YH, Lee MY, Choi YC, Ha Y, Kim H, Kim DY, et al. Elucidation of Relevant Neuroinflammation Mechanisms Using Gene Expression Profiling in Patients with Amyotrophic Lateral Sclerosis. PLoS One 2016;11:e0165290.
7. Yu JH, **Kim M**, Seo JH, Cho S-R. Brain Plasticity and Neurorestoration by Environmental Enrichment. Brain&Neurorehabilitation 2016;9.